

# Axial-vector form factors of the nucleon within the chiral quark-soliton model and their strange components

Antonio Silva,<sup>1,\*</sup> Hyun-Chul Kim,<sup>2,†</sup> Diana Urbano,<sup>1,3,‡</sup> and Klaus Goeke<sup>4,§</sup>

<sup>1</sup>*Centro de Fisica Computacional, Departamento de Fisica da Universidade de Coimbra, P-3004-516 Coimbra, Portugal*

<sup>2</sup>*Department of Physics and Nuclear Physics & Radiation Technology Institute (NuRI), Pusan National University, 609-735 Busan, Republic of Korea*

<sup>3</sup>*Faculdade de Engenharia da Universidade do Porto, R. Dr. Roberto Frias s/n, P-4200-465 Porto, Portugal*

<sup>4</sup>*Institut für Theoretische Physik II, Ruhr-Universität Bochum, D-44780 Bochum, Germany*

(Dated: September 2005)

## Abstract

We investigate three different axial-vector form factors of the nucleon,  $G_A^0$ ,  $G_A^3$ ,  $G_A^8$ , within the framework of the SU(3) chiral quark-soliton model, emphasizing their strangeness content. We take into account the rotational  $1/N_c$  and linear strange quark ( $m_s$ ) contributions using the symmetry-conserving SU(3) quantization and assuming isospin symmetry. The strange axial-vector form factor is also obtained and they all are discussed in the context of the parity-violating scattering of polarized electrons off the nucleon and its relevance to the strange vector form factors.

PACS numbers: 12.40.-y, 14.20.Dh

---

\*Electronic address: ajose@teor.fis.uc.pt

†Electronic address: hchkim@pusan.ac.kr

‡Electronic address: urbano@fe.up.pt

§Electronic address: Klaus.Goeke@tp2.rub.de

## I. INTRODUCTION

Axial-vector properties of the nucleon provide deep insight in understanding its internal structure. For instance, the measured first moment  $I_p$  of the proton spin structure function [1, 2, 3, 4, 5, 6, 7, 8, 9] is directly related to the quark content of the nucleon at a fixed  $Q^2$ :

$$\Gamma_1^p(Q^2) = \int_0^1 g_1^p(x, Q^2) dx = \frac{C_{ns}(Q^2)}{12} a_3 + \frac{C_{ns}(Q^2)}{36} a_8 + \frac{C_s(Q^2)}{9} a_0, \quad (1)$$

where  $g_1^p(x)$  denotes the spin structure function of the proton, and the  $a_i$  are the singlet and non-singlet combinations of the first moments of the parton distributions:

$$\begin{aligned} a_0 &= g_A^0 = \Delta\Sigma = \Delta u + \Delta\bar{u} + \Delta d + \Delta\bar{d} + \Delta s + \Delta\bar{s}, \\ a_3 &= g_A^3 = \Delta u + \Delta\bar{u} - \Delta d - \Delta\bar{d}, \\ a_8 &= g_A^8 = \Delta u + \Delta\bar{u} + \Delta d + \Delta\bar{d} - 2\Delta s - 2\Delta\bar{s}, \end{aligned} \quad (2)$$

and  $C_s$  and  $C_{ns}$  are the first moments of the non-singlet coefficient functions which can be computed in perturbative QCD. The first moments  $a_i$  can be identified as the axial-vector constants  $g_A^i$  in the quark parton model. In particular, the  $g_A^0 = \Delta\Sigma$  is just interpreted in the quark parton model as the fraction of the proton angular momentum carried by the intrinsic spins of the quarks. The  $g_A^3$  and  $g_A^8$  are related to semi-leptonic decays. Thus, the axial-vector constants provide essential information on understanding the spin structure of the nucleon.

Recently, parity-violating asymmetries of the polarized electrons scattered off the nucleon have been intensively measured [10, 11, 12, 13, 14, 15, 16, 17, 18], since two neutral electroweak form factors  $G_E^A$  and  $G_M^Z$  of the proton can be extracted from the asymmetries. Once these form factors are known, one can combine them with  $G_E^\gamma$  and  $G_M^\gamma$  and can disentangle the up, down, and strange quark contributions to the electromagnetic form factors of the nucleon. However, it is also essential to know information on the neutral weak axial-vector form factor,  $G_A^Z$ , defined as

$$G_A^Z(Q^2) = -\tau_3 G_A(Q^2) + G_A^s(Q^2), \quad (3)$$

where  $G_A$  stands for the triplet axial-vector form factor of which the value at  $Q^2 = 0$  is just the axial-vector constant  $g_A^3$  determined from nucleon  $\beta$  decay. Note that  $Q^2$  is the positive four-momentum transfer,  $Q^2 = -q^2$ . The  $G_A^s$  denotes the strange axial-vector form factor and its value at  $Q^2 = 0$  is the strange quark content of the nucleon spin. These axial-vector form factors have been experimentally investigated by quasi-elastic neutrino-nucleon scattering [19] and by pion electroproduction [20]. There a dipole-type parametrization has been used to extract the strange-vector form factors (see Ref. [21] in detail):

$$G_A(Q^2) = \frac{g_A}{(1 + Q^2/M_A^2)^2}, \quad (4)$$

where  $M_A$  is the axial dipole mass. Apparently, the axial-vector properties of the nucleon shed light on the structure of the nucleon in various aspects.

Though a correct theoretical description of the structure of the nucleon should be based on QCD, which would automatically include the excitation of  $q\bar{q}$  pairs in the nucleon, it is

rather difficult to perform in practice such a calculation. It is even very hard to use lattice gauge techniques because they still suffer from technical problems, in particular, in treating light quarks. Thus, we need to use appropriate models which reflect important characteristics of QCD such as chiral symmetry and its spontaneous symmetry breaking and which treat the relevant degrees of freedom in some good approximation. In this sense, the chiral quark-soliton model ( $\chi$ QSM) provides a proper theoretical framework. It is an effective quark theory of QCD in the limit of  $N_c \rightarrow \infty$  concentrating on the instanton-degrees of freedom of the QCD vacuum and resulting in an effective action for valence and sea quarks both moving in a static self-consistent Goldstone background field [22, 23, 24]. The nucleon arises from this effective interaction as a chiral soliton. It has successfully been applied to various properties of the baryons [23] and to forward and generalized parton distributions [25, 26, 27] and has lead even to the prediction of the heavily discussed pentaquark baryon  $\Theta^+$  [28].

The present authors have recently investigated the strange vector form factors [29], utilizing the symmetry-conserving quantization scheme suggested by Praszalowicz *et al.* [30]. We predicted the SAMPLE, HAPPEX, A4, and G0 experiments [29, 31]. Results have shown a fairly good agreement with experimental data of the A4, SAMPLE, and HAPPEX. However, since the experimental uncertainties are rather large, it is hard to judge any theoretical calculation. While the extracted strange vector form factors appear to have large experimental uncertainties, the parity-violating asymmetries are measured with relatively good precision. Thus, the parity-violating asymmetries may be more reliable to justify the model descriptions.

In the present work, we want to study all three axial-vector form factors within the framework of the  $\chi$ QSM, focusing on the strangeness content of the nucleon. In fact, axial-vector properties of the nucleon have to some extent already been studied in the SU(2) and SU(3)  $\chi$ QSM, previously [32, 33, 34, 35, 36, 37, 38, 39, 40]. However, these studies were not complete and some of them did not use the symmetry conserving quantization method [30], which guarantees that the Gell-Mann-Nishijima relations are obeyed. Hence, we will calculate all axial-vector form factors in this work, employing the symmetry-conserving quantization. We will follow also the same set of parameters we used for deriving the strange vector form factors so that the parity-violating asymmetries may be studied [41].

This paper is organized as follows: In Section II, we briefly show how to derive the axial-vector form factors in the  $\chi$ QSM. In Section III, we present the results and discuss them. In Section IV, we summarize and draw the conclusion of the present work.

## II. AXIAL-VECTOR FORM FACTORS IN THE $\chi$ QSM

In the present section we briefly mention the general expression for the axial-vector form factors in the  $\chi$ QSM (see also reviews [22, 23]).

The axial-vector form factors are expressed in terms of the following quark matrix elements:

$$\langle N(p', S'_3) | A_\mu^{(x)} | N(p, S_3) \rangle = \bar{u}_N(p', S'_3) \left[ \gamma_\mu \gamma_5 G_A^{(x)}(q^2) + i \gamma_5 \frac{q^\nu}{2M_N} G_P^{(x)}(q^2) \right] u_N(p, S_3), \quad (5)$$

where  $G_A^{(x)}(q^2)$  and  $G_P^{(x)}(q^2)$  are the axial-vector and induced pseudoscalar form factors, respectively. Note that we ignore the form factor of the second kind, *i.e.* the induced pseudotensor form factor, since it is irrelevant to the present work. The  $q^2$  is the square of

the four momentum transfer  $q^2 = -Q^2$  with  $Q^2 > 0$ . The  $M_N$  and  $u_N(p, S_3)$  stand for the nucleon mass and its spinor with the third component of the nucleon spin, respectively. The axial-vector quark current  $A_\mu^{(\chi)}$  can be expressed in Euclidean space as follows:

$$A_\mu^{(\chi)}(x) = -i\psi^\dagger(x)\gamma_\mu\gamma_5\frac{\lambda^\chi}{2}\psi(x), \quad (6)$$

where  $\lambda^\chi$  are the Gell-Mann matrices.

Since we are interested in the axial-vector form factors of the nucleon in low-energy regions ( $Q^2 \leq 1 \text{ GeV}^2$ ), we will work in the Breit frame, where the time component of the axial-vector current vanishes. Thus, the axial-vector form factors can be related only to the space component of the axial-vector current. This is no real restriction since its time component is suppressed in the large  $N_c$  limit, compared to the spatial one. Having carried out a tedious but straightforward calculation following Refs.[23, 42, 43], we derive the expressions for the triplet ( $\chi = 3$ ) and octet ( $\chi = 8$ ) axial-vector densities of the nucleon:

$$\begin{aligned} G_A^{(\chi)}(q^2) &= \frac{M}{E} \int d^3x [j_0(|\mathbf{q}|r) \langle N(S_3) | A^{3\chi}(\mathbf{x}) | N(S_3) \rangle \\ &\quad - \sqrt{2\pi} j_2(|\mathbf{q}|r) \langle N(S_3) | \{\mathbf{Y}_2(\hat{\mathbf{r}}) \otimes \mathbf{A}_1^\chi(\mathbf{x})\}_{10} | N(S_3) \rangle] \\ &= \frac{M}{E} \int r^2 dr \left[ j_0(|\mathbf{Q}|r) A_0^{\chi,B}(r) - \frac{1}{\sqrt{2}} j_2(|\mathbf{Q}|r) A_2^{\chi,B}(r) \right], \end{aligned} \quad (7)$$

where

$$A_0^{\chi,B}(r) = \int d\Omega \langle N(S_3) | A^{3\chi}(\mathbf{x}) | N(S_3) \rangle, \quad (8)$$

$$A_2^{\chi,B}(r) = \int d\Omega \langle N(S_3) | \left\{ \sqrt{4\pi} \mathbf{Y}_2(\hat{\mathbf{r}}) \otimes \mathbf{A}_1^\chi(\mathbf{x}) \right\}_{10} | N(S_3) \rangle. \quad (9)$$

Here  $E$  is the on-shell energy of the nucleon,  $E = \sqrt{M_N^2 + \mathbf{q}^2/4}$ . The  $j_0(|\mathbf{Q}|r)$  and  $j_2(|\mathbf{Q}|r)$  denote the spherical Bessel functions. The  $A^{3\chi}$  is the third component of the axial-vector current in Eq.(6) and the  $\mathbf{Y}_2$  denotes the second-rank spherical tensors.

Having carried out the symmetry conserving collective quantization with the linear  $m_s$  corrections as well as rotational  $1/N_c$  corrections taken into account, we end up with the following expressions for Eq.(8):

$$\begin{aligned} &\langle N(S_3) | A^{3\chi=3,8}(\mathbf{z}) | N(S_3) \rangle \\ &= \frac{1}{3} \left\langle D_{\chi^3}^{(8)} \right\rangle_N \mathcal{A}_0(\mathbf{z}) + \frac{1}{3\sqrt{3}I_1} \left( \left\langle J_3 D_{\chi^8}^{(8)} \right\rangle_N - 2K_1 m_8 \left\langle D_{83}^{(8)} D_{\chi^8}^{(8)} \right\rangle_N \right) \mathcal{B}_0(\mathbf{z}) \\ &\quad + \frac{1}{3I_2} \left( \left\langle d_{3ab} D_{\chi^a}^{(8)} J_b \right\rangle_N - 2K_2 m_8 \left\langle D_{8a}^{(8)} D_{\chi^b}^{(8)} d_{ab3} \right\rangle_N \right) \mathcal{C}_0(\mathbf{z}) - \frac{i}{6I_1} \left\langle D_{\chi^3}^{(8)} \right\rangle_N \mathcal{D}_0(\mathbf{z}) \\ &\quad + \frac{2}{3} \left( m_0 \left\langle D_{\chi^3}^{(8)} \right\rangle_N + \frac{1}{\sqrt{3}} m_8 \left\langle D_{88}^{(8)} D_{\chi^3}^{(8)} \right\rangle_N \right) \mathcal{H}_0(\mathbf{z}) \\ &\quad + \frac{2}{3\sqrt{3}} m_8 \left\langle D_{83}^{(8)} D_{\chi^8}^{(8)} \right\rangle_N \mathcal{I}_0(\mathbf{z}) + \frac{2}{3} m_8 \left\langle D_{8a}^{(8)} D_{\chi^b}^{(8)} d_{ab3} \right\rangle_N \mathcal{J}_0(\mathbf{z}), \\ &\langle N(S_3) | A^{3\chi=0}(\mathbf{x}) | N(S_3) \rangle \\ &= \frac{2}{3I_1} \left( \left\langle J_3 \right\rangle_N - K_1 m_8 \left\langle D_{83}^{(8)} \right\rangle_N \right) \mathcal{B}_0(\mathbf{z}) + \frac{2}{3} m_8 \left\langle D_{83}^{(8)} \right\rangle_N \mathcal{I}_0(\mathbf{z}), \end{aligned} \quad (10)$$

where  $I_i$  and  $K_i$  are the moments of inertia of the soliton. The  $m_0$  and  $m_8$  denote the singlet and octet components of the quark mass matrix:  $m_0 = (2\bar{m} + m_s)/3$  and  $m_8 = (\bar{m} - m_s)/\sqrt{3}$  with  $\bar{m} = m_u = m_d$ , respectively. The  $d_{ab3}$  is the totally symmetric tensor in SU(3). The  $D^{(8)}$  represent the SU(3) Wigner functions and  $\langle \rangle_N$  stand for their matrix elements sandwiched between the collective nucleon wave functions. These matrix elements are finally expressed in terms of the SU(3) Clebsch-Gordan coefficients. Note that here we tacitly have considered the wave function corrections arising from SU(3)-symmetry breaking, which mixes the pure nucleon state with states in higher representations. The nucleon state  $J_3$  is the third component of the spin operator. The explicit expressions for the quark densities,  $\mathcal{A}_0$ ,  $\mathcal{B}_0$ ,  $\mathcal{C}_0$ ,  $\mathcal{D}_0$ ,  $\mathcal{H}_0$ ,  $\mathcal{I}_0$ , and  $\mathcal{J}_0$  can be found in Appendix.

Note that the matrix element  $\langle N(S_3) | \{ \mathbf{Y}_2(\hat{\mathbf{r}}) \otimes \mathbf{A}_1^{x=0}(\mathbf{x}) \}_{10} | N(S_3) \rangle$  in Eq.(9) can be put into the same form as Eq.(10), except for replacing the operators in Eq.(10) by others which are given in Table I. Actually, in flavor SU(2), the above SU(3) expressions are reduced to the isoscalar and isovector ones as follows:

$$A_0^{x=0}(r) = A_0^{T=0} = \frac{1}{3I_1} \langle J_3 \rangle_N \mathcal{B}_0(r), \quad (11)$$

$$A_0^{x=3}(r) = A_0^{T=3} = -\frac{1}{\sqrt{3}} \langle D_{33}^{(3)} \rangle_N \mathcal{A}_0(r) - \frac{1}{3\sqrt{2}I_1} \langle D_{33}^{(3)} \rangle_N \mathcal{D}_0(r), \quad (12)$$

where the operators required for the function  $A_2(r)$  in SU(2) can be read out from Table I.

Densities	Operators
$\mathcal{B}_0, \mathcal{I}_0$	$\boldsymbol{\sigma}$
$\mathcal{B}_2, \mathcal{I}_2$	$\{ \sqrt{4\pi} Y_2 \otimes \sigma_1 \}_1$
$\mathcal{A}_0, \mathcal{C}_0, \mathcal{H}_0, \mathcal{J}_0$	$\boldsymbol{\sigma} \cdot \boldsymbol{\tau}$
$\mathcal{A}_2, \mathcal{C}_2, \mathcal{H}_2, \mathcal{J}_2$	$-\sqrt{3} \{ \{ \sqrt{4\pi} Y_2 \otimes \sigma_1 \}_1 \otimes \tau_1 \}_0$
$\mathcal{D}_0$	$\boldsymbol{\sigma} \times \boldsymbol{\tau}$
$\mathcal{D}_2$	$-i\sqrt{2} \{ \{ \sqrt{4\pi} Y_2 \otimes \sigma_1 \}_1 \otimes \tau_1 \}_1$

TABLE I: This table shows how to obtain  $A_2^{x,B}(r)$  by replacing operators. The factor  $-\sqrt{3}$  comes from  $\boldsymbol{\sigma} \cdot \boldsymbol{\tau} = -\sqrt{3} \{ \sigma_1 \otimes \tau_1 \}_0$  and  $-i\sqrt{2}$  from  $\boldsymbol{\sigma} \times \boldsymbol{\tau} = -i\sqrt{2} \{ \sigma_1 \otimes \tau_1 \}_1$ .

Now, we turn to the flavor decomposition of the axial-vector form factors. The flavor axial-vector form factors can be expressed in terms of the singlet and non-singlet ones as follows:

$$\begin{aligned} G_A^u &= \frac{1}{3}G_A^0 + \frac{1}{2}G_A^3 + \frac{1}{2\sqrt{3}}G_A^8, \\ G_A^d &= \frac{1}{3}G_A^0 - \frac{1}{2}G_A^3 + \frac{1}{2\sqrt{3}}G_A^8, \\ G_A^s &= \frac{1}{3}G_A^0 - \frac{1}{\sqrt{3}}G_A^8. \end{aligned} \quad (13)$$

The fractions of the nucleon angular momentum carried by the intrinsic spin of the quarks with given flavors are just identified as the flavor components of the axial-vector form factors at  $Q^2 = 0$ :

$$\Delta u + \Delta \bar{u} = G_A^u(Q^2 = 0), \quad \Delta d + \Delta \bar{d} = G_A^d(Q^2 = 0), \quad \Delta s + \Delta \bar{s} = G_A^s(Q^2 = 0). \quad (14)$$

### III. RESULTS AND DISCUSSION

We present now the results obtained from the  $\chi$ QSM. A detailed description of the numerical techniques to solve the model can be found, for example, in Refs. [23, 42]. The parameters of the model comprise the constituent quark mass  $M$ , the current quark mass  $m_u = m_d$ , the cut-off  $\Lambda$  of the proper-time regularization, and the strange quark mass  $m_s$ . These parameters are not free but are adjusted to independent observables in a very clear way. In fact, this was done many years ago: The  $\Lambda$  and the  $m_u$  are fixed to a given  $M$  in the mesonic sector. The physical pion mass  $m_\pi = 139$  MeV and the pion decay constant  $f_\pi = 93$  MeV are reproduced by these parameters. The strange quark mass is chosen to be  $m_s = 180$  MeV throughout the present work. The remaining parameter  $M$  is varied from 400 MeV to 450 MeV. However, the value of 420 MeV, which for many years is known to produce the best fit to many baryonic observables [23], is selected for the present result.

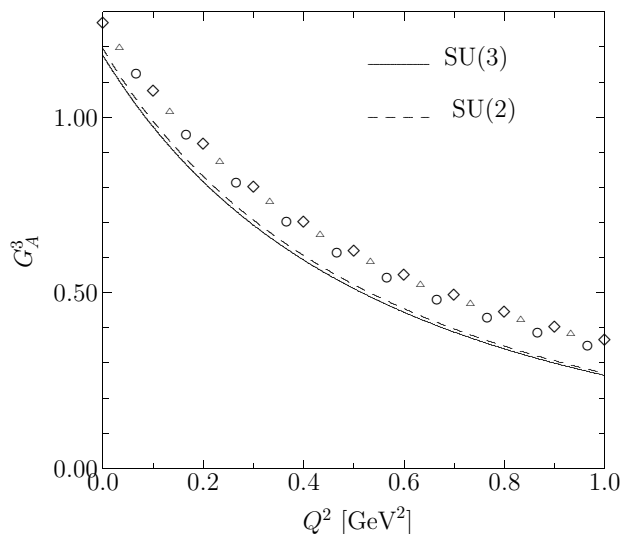


FIG. 1: The triplet axial-vector form factor,  $G_A^3$  as a function of  $Q^2$ . The solid curve depicts the result of the  $\chi$ QSM in the SU(3) version, while the dashed one draws  $G_A$  from the SU(2) calculation. The constituent quark mass is  $M = 420$  MeV. The open circles, squares, and triangles represent the results with the dipole-type parametrization of the  $G_A^3$  with given empirical values of the axial-vector mass  $M_A$ .

Figure 1 depicts the results of the triplet axial-vector form factors  $G_A = G_A^3$ . The solid curve draws  $G_A(Q^2)$  from the SU(3) model, whereas the dashed one does its SU(2) result. The open circles, squares, and triangles represent the results based on Eq.(4) with three different well-known average axial-vector masses:  $M_A = 1.032 \pm 0.036$  GeV from neutrino (antineutrino) scattering experiments on protons and nuclei [19],  $M_A = 1.069 \pm 0.016$  GeV from pion electroproduction, and  $M_A = 1.077 \pm 0.039$  from charged pion electroproduction [20], respectively. In all these experimental analyses, the value  $g_A = 1.2673 \pm 0.0035$  known from  $\beta$ -decay [44] was used for the value of  $G_A$  at  $Q^2 = 0$ . The  $G_A$  from the SU(3)  $\chi$ QSM does almost coincide with that of the SU(2) one. The theoretical SU(3) value is  $g_A = 1.176$ . Thus the SU(3) result is different from the experimental data by only 8%. Compared to the empirical dipole type  $G_A$ , the results in Figure 1 show a very similar  $Q^2$ -dependence.

The axial-vector radii are defined as

$$\langle r_\chi^2 \rangle_A = -6 \frac{1}{G_A^{(\chi)}(0)} \left. \frac{dG_A(Q^2)}{dQ^2} \right|_{Q^2=0}, \quad (15)$$

from which we obtain the triplet axial-vector radius of the SU(3)  $\chi$ QSM :  $\langle r_3^2 \rangle_A^{1/2} = 0.732$  fm. The experimental data is given as  $\langle r_3^2 \rangle_A^{1/2} = 0.635 \pm 0.023$  fm[20]. Thus, the triplet axial-vector radius from the model is also comparable to the data with a deviation of less than 15%. The axial-vector dipole mass can be obtained from Eq. (15) as follows:

$$M_A^2 = 12 / \langle r_3^2 \rangle_A. \quad (16)$$

We obtain for the axial-vector dipole mass of SU(3)  $\chi$ QSM:  $M_A = 0.934$  GeV. Compared to the empirical values mentioned above, the axial-vector dipole mass from the SU(3)  $\chi$ QSM calculation deviates from the exmpirical ones by about  $\pm(10 \sim 15) \%$ .

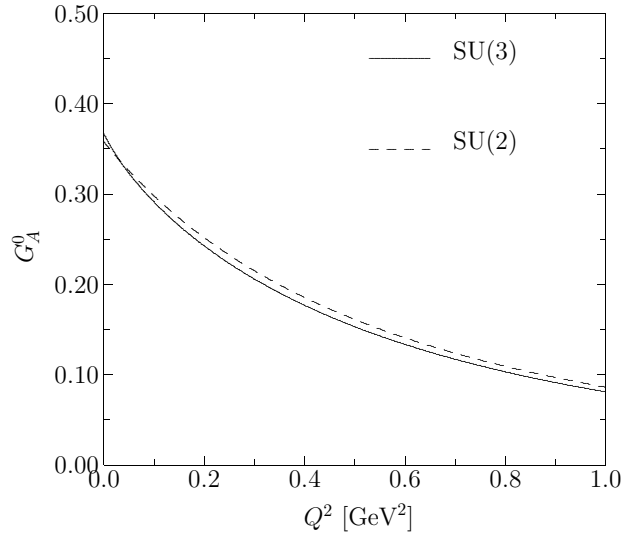


FIG. 2: The singlet axial-vector form factor,  $G_A^0$  as a function of  $Q^2$ . The solid curve depicts the result of the SU(3)  $\chi$ QSM model, while the dashed one draws  $G_A$  from the SU(2) calculation. The constituent quark mass is  $M = 420$  MeV.

Figure 2 draws the results of the singlet axial-vector form factors. The general tendency is similar to the case of  $G_A^3$ . The SU(2) result is almost the same as that from the SU(3)  $\chi$ QSM as in the case of  $G_A^3$ . Figure 3 represents the results of the octet axial-vector form factors. Note that in SU(2)  $G_A^8$  is not defined.

The singlet axial-vector constant  $g_A^0 = G_A^0(Q^2 = 0)$  provides information on the nucleon angular momentum carried by the intrinsic spin of the light quarks as defined in Eq.(2). It can be determined from the proton and neutron structure function. The  $g_A^0$  can be extracted from longitudinally polarized deep-inelastic lepton scattering experiments and is known approximately [46] to be  $0.2 \sim 0.35$ . However, note that  $g_A^0$  includes in general the gluonic content of the nucleon spin which is experimentally not well known. From the present results, we get  $g_A^0 = 0.37$ .

As for the octet axial-vector constant, it is related to semileptonic decays and known experimentally to be  $g_A^8 = 0.338 \pm 0.015$  [45]. As shown in Fig. 3, we obtain  $g_A^8 = 0.36$  which is in a remarkable agreement with the experimental data.

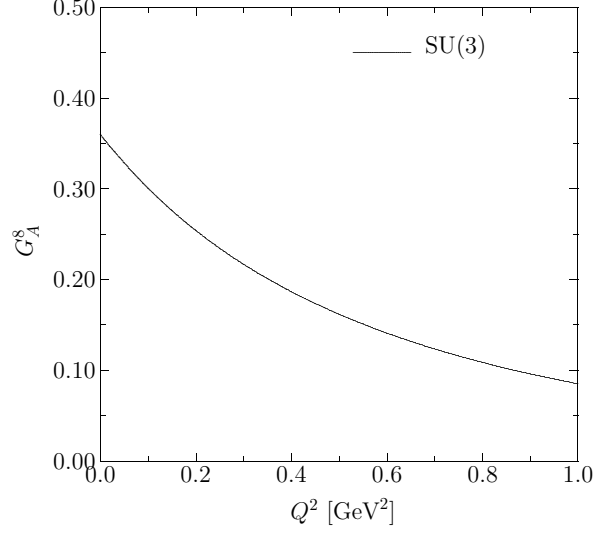


FIG. 3: The octet axial-vector form factor,  $G_A^8$  as a function of  $Q^2$ . The solid curve depicts the result of the SU(3) model. The constituent quark mass is  $M = 420$  MeV.

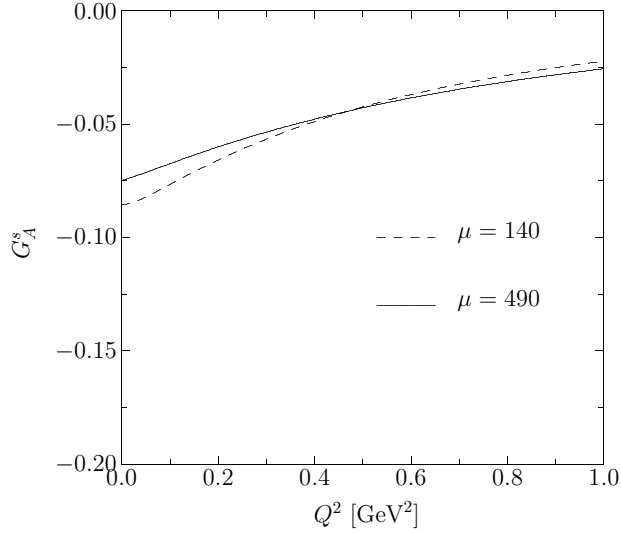


FIG. 4: The strange axial-vector form factor,  $G_A^s$  as a function of  $Q^2$ . The solid curve and dashed curves depict the results for the kaon ( $\mu = 490$  MeV) and pion ( $\mu = 140$  MeV) asymptotic tails, respectively. The constituent quark mass is  $M = 420$  MeV.

Figure 4 depicts the strange axial-vector form factor. Actually two curves are given the difference of which is a measure for the systematic error of  $G_A^s(Q^2)$ . The reasoning for that has been discussed in Ref. [29, 31] and can shortly be summarized as follows: The SU(3) soliton is constructed by embedding the SU(2) one into the SU(3):

$$U_{\text{SU}(3)} = \begin{pmatrix} U_{\text{SU}(2)} & 0 \\ 0 & 1 \end{pmatrix}, \quad (17)$$

with the SU(2) hedgehog given by

$$U_{\text{SU}(2)} = \exp[i\gamma_5 \mathbf{n} \cdot \boldsymbol{\tau} P(r)]. \quad (18)$$



The profile function  $P(r)$  is found by minimizing the classical energy of the soliton in a self-consistent way. While the SU(2) soliton incorporates the asymptotic pion behavior  $\exp(-m_\pi r)/r$  naturally, the SU(3) hedgehog by the embedding the SU(2) soliton renders all other pseudo-Goldstone bosons have the same asymptotic behavior by construction. Therefore, this treatment is phenomenologically unsatisfactory, in particular, when we deal with quantities related to solely strange quarks. Thus, we will consider here the kaonic asymptotic tail for the profile function and look at the interval spanned by results of the more consistent pion asymptotics and the phenomenologically driven kaon asymptotics of  $P(r)$  as giving an idea of the systematic model uncertainties stemming from the lack of exact treatment of the SU(3) meson asymptotics. It is interesting to see that for  $G_A^s(Q^2)$  the result with the kaon tail does not differ much from that with the pion one, which was not the case for the strange vector form factors  $G_M^s(Q^2)$  and  $G_E^s(Q^2)$  [29, 31]. It implies that the strange axial-vector form factor is insensitive to the asymptotic part of the axial-vector densities.

	SU(2)	SU(3)	[46]
$\Delta u + \Delta \bar{u}$	0.777	0.814	$0.78 \pm 0.03$
$\langle r_u^2 \rangle^{1/2}$	0.665	0.751	
$\Delta d + \Delta \bar{d}$	-0.419	-0.362	$-0.48 \pm 0.03$
$\langle r_d^2 \rangle^{1/2}$	0.668	0.688	
$\Delta s + \Delta \bar{s}$	-	-0.086 (-0.075)	$-0.14 \pm 0.03$
$\langle r_s^2 \rangle^{1/2}$	-	0.554 (0.172)	

TABLE II: Results for the fractions of the nucleon carried by quarks and flavor axial-vector radii. Model parameters are  $M = 420$  MeV and  $m_s = 180$  MeV. The calculations are performed with the profile function having a pion-tail. For the purely strange quantities the results with the kaon tail are given in brackets for comparison.

In Table II, we list the results for each flavor contribution to the nucleon spin and the flavor axial-vector radii. Compared to the empirical results [46], it is found that the results of this work for  $\Delta q_i + \Delta \bar{q}_i$  are slightly deviating from them by about  $20 \sim 25\%$  in general apart from  $\Delta s + \Delta \bar{s}$ . However, note that those data in Ref. [46] are extracted assuming SU(3) symmetry. This assumption has been shown by some of the present authors in Ref. [40] to cause error bars for  $\Delta s + \Delta \bar{s}$  very much larger than those given in Ref. [46].

#### IV. SUMMARY AND CONCLUSION

In the present work, we have investigated the singlet and non-singlet axial-vector form factors within the framework of the SU(3) chiral quark-soliton model, incorporating the symmetry-conserving quantization. The rotational  $1/N_c$  and strange quark mass  $m_s$  corrections were taken into account. We have used the same set of parameters for the present investigation so that we may utilize the present results in a future study on the parity-violating asymmetries of the polarized electron scatterings off the proton. The results of the singlet and triplet axial-vector form factors turned out to be almost the same as that with those in SU(2). In order to see the sensitivity to the asymptotics of the soliton, we employed pion and kaon tails for the strange axial-vector form factors, as was done in Ref. [29, 31].

While the strange vector form factors are rather sensitive [29, 31], the axial-vector one is not.

	SU(2)	SU(3)	Exp.
$g_A^0$	0.358	0.367	
$\langle r_0^2 \rangle^{1/2}$	0.662	0.844	
$M_A^0$	1.033	0.810	
$g_A^3$	1.196	1.176	$1.267 \pm 0.004$ [44]
$\langle r_3^2 \rangle^{1/2}$	0.666	0.732	$0.635 \pm 0.023$ [20]
$M_A$	1.026	0.934	$1.077 \pm 0.039$ [20]
$g_A^8$	—	0.360	
$\langle r_8^2 \rangle^{1/2}$	—	0.739	
$M_A^8$	—	0.926	
$g_A^s$	—	$-0.086$ ( $-0.075$ )	$-0.14 \pm 0.03$ [46]
$\langle r_s^2 \rangle^{1/2}$	—	$0.554$ ( $0.172$ )	

TABLE III: Axial-vector constants  $g_A^\chi = G_A^{(\chi)}(Q^2 = 0)$ ,  $g_A^s$ , axial-vector radii (in fm) (Eq. 15), and dipole axial-vector masses (in GeV) from the dipole expression. Model parameters are  $M = 420$  MeV and  $m_s = 180$  MeV. The calculations are performed with the profile function having a pion-tail. For the purely strange quantities the results with the kaon tail are given in brackets for comparison.

The results of the axial-vector constants, corresponding radii, and the dipole axial-vector masses are summarized in Table III. The present results are in general good agreement with the existing experimental data.

The present investigation possesses one noticeable virtue: Since we are able to calculate the axial-vector form factors together with the strange electromagnetic ones within the same scheme, we can directly get access to the electroweak interactions of the proton. In order to calculate the parity-violating asymmetries of the polarized electrons scattered off the proton, we must have all required form factors derived consistently. Actually, combining the present results of the axial-vector form factors together with the strange vector form factors, we can proceed to delve into the parity-violating asymmetries. Since the parity-violating asymmetries have been and will be measured in different kinematical regions with a good precision, they will provide a criterion for theoretical works.

The parity-violating asymmetries of polarized electron-proton scattering is presently under investigation.

## Acknowledgments

AS acknowledges partial financial support from the Portugese Praxis XXI/BD/15681/98. The work has also been supported by Korean-German grant of the Deutsche Forschungsgemeinschaft and KOSEF (F01-2004-000-00102-0). The work is partially supported by

the Transregio-Sonderforschungsbereich Bonn-Bochum-Giessen as well as by the Verbundforschung and the International Office of the Federal Ministry for Education and Research (BMBF).

## APPENDIX A: DENSITIES

In this Appendix, we provide the densities for the axial-vector form factors given in Eq.(10). The sums run freely over all single-quark levels including the valence one, except the sum over  $m_0$ , which is restricted to negative-energy orbits:

$$\frac{1}{N_c} \mathcal{A}_0(z) = \langle \text{val} | z \rangle \boldsymbol{\sigma} \cdot \boldsymbol{\tau} \langle z | \text{val} \rangle + \sum_n \mathcal{R}_1(\varepsilon_n) \langle n | z \rangle \boldsymbol{\sigma} \cdot \boldsymbol{\tau} \langle z | n \rangle \quad (\text{A1})$$

$$\begin{aligned} \frac{1}{N_c} \mathcal{B}_0(z) &= \sum_{m \neq 0} \frac{1}{\varepsilon_{\text{val}} - \varepsilon_m} \langle \text{val} | z \rangle \boldsymbol{\sigma} \langle z | m \rangle \cdot \langle \text{val} | \boldsymbol{\tau} | m \rangle \\ &\quad - \frac{1}{2} \sum_{n,m} \mathcal{R}_2(\varepsilon_n, \varepsilon_m) \langle n | z \rangle \boldsymbol{\sigma} \langle z | m \rangle \cdot \langle n | \boldsymbol{\tau} | m \rangle \end{aligned} \quad (\text{A2})$$

$$\begin{aligned} \frac{1}{N_c} \mathcal{C}_0(z) &= \sum_{m^0} \frac{1}{\varepsilon_{\text{val}} - \varepsilon_{m^0}} \langle \text{val} | z \rangle \boldsymbol{\sigma} \cdot \boldsymbol{\tau} \langle z | m^0 \rangle \langle m^0 | \text{val} \rangle \\ &\quad - \sum_{n,m^0} \mathcal{R}_2(\varepsilon_n, \varepsilon_{m^0}) \langle n | z \rangle \boldsymbol{\sigma} \cdot \boldsymbol{\tau} \langle z | m^0 \rangle \langle m^0 | n \rangle \end{aligned} \quad (\text{A3})$$

$$\begin{aligned} \frac{1}{N_c} \mathcal{D}_0(z) &= \sum_n \frac{\text{sgn}(\varepsilon_n)}{\varepsilon_{\text{val}} - \varepsilon_n} \langle n | z \rangle \boldsymbol{\sigma} \times \boldsymbol{\tau} \langle z | \text{val} \rangle \cdot \langle \text{val} | \boldsymbol{\tau} | n \rangle \\ &\quad + \frac{1}{2} \sum_{n,m} \mathcal{R}_3(\varepsilon_n, \varepsilon_m) \langle m | z \rangle \boldsymbol{\sigma} \times \boldsymbol{\tau} \langle z | n \rangle \cdot \langle n | \boldsymbol{\tau} | m \rangle \end{aligned} \quad (\text{A4})$$

$$\begin{aligned} \frac{1}{N_c} \mathcal{H}_0(z) &= \sum_{n \neq 0} \frac{1}{\varepsilon_{\text{val}} - \varepsilon_n} \langle \text{val} | z \rangle \boldsymbol{\sigma} \cdot \boldsymbol{\tau} \langle z | n \rangle \langle n | \gamma^0 | \text{val} \rangle \\ &\quad + \frac{1}{2} \sum_{n,m} \mathcal{R}_4(\varepsilon_n, \varepsilon_m) \langle m | z \rangle \boldsymbol{\sigma} \cdot \boldsymbol{\tau} \langle z | n \rangle \langle n | \gamma^0 | m \rangle \end{aligned} \quad (\text{A5})$$

$$\begin{aligned} \frac{1}{N_c} \mathcal{I}_0(z) &= \sum_{n \neq 0} \frac{1}{\varepsilon_{\text{val}} - \varepsilon_n} \langle \text{val} | z \rangle \boldsymbol{\sigma} \langle z | n \rangle \cdot \langle n | \gamma^0 \boldsymbol{\tau} | \text{val} \rangle \\ &\quad + \frac{1}{2} \sum_{n,m} \mathcal{R}_4(\varepsilon_n, \varepsilon_m) \langle m | z \rangle \boldsymbol{\sigma} \langle z | n \rangle \cdot \langle n | \gamma^0 \boldsymbol{\tau} | \text{val} \rangle \end{aligned} \quad (\text{A6})$$

$$\begin{aligned} \frac{1}{N_c} \mathcal{J}_0(z) &= \sum_{m^0} \frac{1}{\varepsilon_{\text{val}} - \varepsilon_{m^0}} \langle \text{val} | z \rangle \boldsymbol{\sigma} \cdot \boldsymbol{\tau} \langle z | m^0 \rangle \langle m^0 | \gamma^0 | \text{val} \rangle \\ &\quad + \sum_{n,m^0} \mathcal{R}_4(\varepsilon_n, \varepsilon_{m^0}) \langle n | z \rangle \boldsymbol{\sigma} \cdot \boldsymbol{\tau} \langle z | m^0 \rangle \langle m^0 | \gamma^0 | n \rangle \end{aligned} \quad (\text{A7})$$

with the regularization functions

$$\mathcal{R}_1(\varepsilon_n) = -\frac{\varepsilon_n}{2\sqrt{\pi}} \int_{1/\Lambda^2}^{\infty} \frac{du}{\sqrt{u}} e^{-u\varepsilon_n^2},$$

$$\begin{aligned}
\mathcal{R}_2(\varepsilon_n, \varepsilon_m) &= \frac{1}{2} \frac{\text{sgn}(\varepsilon_m) - \text{sgn}(\varepsilon_n)}{\varepsilon_n - \varepsilon_m}, \\
\mathcal{R}_3(\varepsilon_n, \varepsilon_m) &= \frac{1}{2\pi} \int_{1/\Lambda^2}^{\infty} dw \int_0^1 d\beta \frac{(1-\beta)\varepsilon_n - \beta\varepsilon_m}{\sqrt{(1-\beta)\beta}} e^{-[\varepsilon_n^2(1-\beta) + \varepsilon_m^2\beta]w}, \\
\mathcal{R}_4(\varepsilon_n, \varepsilon_m) &= \frac{1}{2\sqrt{\pi}} \int_{1/\Lambda^2}^{\infty} \frac{du}{\sqrt{u}} \frac{\varepsilon_m e^{-\varepsilon_m^2 u} - \varepsilon_n e^{-\varepsilon_n^2 u}}{\varepsilon_n - \varepsilon_m}.
\end{aligned} \tag{A8}$$

- 
- [1] J. Ashman *et al.*, Nucl. Phys. B **328**, 1 (1989).
  - [2] B. Adeva *et al.*, Phys. Lett. B **302**, 533 (1993).
  - [3] D. Adams *et al.*, Phys. Lett. B **329** 399 (1994).
  - [4] P.L. Anthony *et al.*, Phys. Rev. Lett. **71**, 959 (1993).
  - [5] K. Abe *et al.*, Phys. Rev. Lett. **75** (1995) 25.
  - [6] K. Abe *et al.* [E154 Collaboration], Phys. Lett. B **405**, 180 (1997) [arXiv:hep-ph/9705344].
  - [7] A. Airapetian *et al.* [HERMES Collaboration], Phys. Lett. B **442**, 484 (1998) [arXiv:hep-ex/9807015].
  - [8] P. L. Anthony *et al.* [E155 Collaboration], Phys. Lett. B **463**, 339 (1999) [arXiv:hep-ex/9904002].
  - [9] P. L. Anthony *et al.* [E155 Collaboration], neutron spin structure functions g1(p) and g1(n),” Phys. Lett. B **493** (2000) 19.
  - [10] B. Mueller *et al.* [SAMPLE Collaboration], Phys. Rev. Lett. **78** (1997) 3824.
  - [11] D. T. Spayde *et al.* [SAMPLE Collaboration], Phys. Rev. Lett. **84** (2000) 1106.
  - [12] R. Hasty *et al.* [SAMPLE Collaboration], Science **290** (2000) 2117.
  - [13] K. A. Aniol *et al.* [HAPPEX Collaboration], Phys. Lett. **509B** (2001) 211.
  - [14] F. E. Maas *et al.* [A4 Collaboration], Eur. Phys. J. A **17** (2003) 339; Phys. Rev. Lett. **93** (2004) 022002.
  - [15] K. A. Aniol *et al.* [HAPPEX Collaboration], Phys. Rev. C **69** (2004) 065501.
  - [16] K. A. Aniol *et al.* [HAPPEX Collaboration], arXiv:nucl-ex/0506010.
  - [17] K. A. Aniol *et al.* [HAPPEX Collaboration], arXiv:nucl-ex/0506011.
  - [18] D. S. Armstrong *et al.* [G0 Collaboration], arXiv:nucl-ex/0506021.
  - [19] T. Kitagaki *et al.*, Phys. Rev. D **28** (1983) 436.
  - [20] A. Liesenfeld *et al.* [A1 Collaboration], Phys. Lett. B **468** (1999) 20 [arXiv:nucl-ex/9911003].
  - [21] E. J. Beise, Eur. Phys. J. A **24S2**, 43 (2005) [arXiv:nucl-ex/0501019].
  - [22] D. Diakonov, V. Y. Petrov and P. V. Pobylitsa, Nucl. Phys. **B306** (1988) 809.
  - [23] C. V. Christov *et al.*, Prog. Part. Nucl. Phys. **37** (1996) 91.
  - [24] R. Alkofer, H. Reinhardt and H. Weigel, Phys. Rept. **265** (1996) 139.
  - [25] D. Diakonov, V. Petrov, P. Pobylitsa, M. V. Polyakov and C. Weiss, Nucl. Phys. **B480** (1996) 341.
  - [26] V. Y. Petrov, P. V. Pobylitsa, M. V. Polyakov, I. Bornig, K. Goeke and C. Weiss, Phys. Rev. **D57** (1998) 4325.
  - [27] K. Goeke, M. V. Polyakov and M. Vanderhaeghen, Prog. Part. Nucl. Phys. **47** (2001) 401.
  - [28] D. Diakonov, V. Petrov, and M. V. Polyakov, Z. Phys. A **359**, 305 (1997)
  - [29] A. Silva, H.-Ch. Kim and K. Goeke, Phys. Rev. D **65** (2002) 014016; D **66** (2002) 039902 (E).

- [30] M. Praszalowicz, T. Watabe and K. Goeke, Nucl. Phys. **A647** (1999) 49.
- [31] A. Silva, H.-Ch. Kim and K. Goeke, Eur. Phys. J. A **22**, 481 (2004)
- [32] M. Wakamatsu, Phys. Lett. B **234**, 223 (1990).
- [33] M. Wakamatsu and T. Watabe, Phys. Lett. B **312**, 184 (1993).
- [34] C. V. Christov, A. Blotz, K. Goeke, P. Pobylitsa, V. Petrov, M. Wakamatsu and T. Watabe, Phys. Lett. B **325**, 467 (1994).
- [35] R. Alkofer and H. Weigel, Phys. Lett. B **319**, 1 (1993) [arXiv:hep-ph/9308327].
- [36] C. V. Christov, K. Goeke and P. V. Pobylitsa, Phys. Rev. C **52**, 425 (1995).
- [37] T. Watabe, C. V. Christov and K. Goeke, arXiv:hep-ph/9506440.
- [38] A. Blotz, M. Praszalowicz, and K. Goeke, Phys. Lett. B **317**, 195 (1993).
- [39] A. Blotz, M. Praszalowicz and K. Goeke, Phys. Rev. D **53**, 485 (1996). [arXiv:hep-ph/9403314].
- [40] H.-Ch. Kim, M. Praszalowicz, and K. Goeke, Phys. Rev. D **61**, 114006 (1996).
- [41] A. Silva, H.-Ch. Kim and K. Goeke, PNU-NTG-11/2005, RUB-TPII-09/2005 (2005).
- [42] H.-Ch. Kim, A. Blotz, M. V. Polyakov and K. Goeke, Phys. Rev. **D53** (1996) 4013.
- [43] A. Silva, Ph.D. Thesis (unpublished) (2004).
- [44] S. Eidelman *et al.* [Particle Data Group], Phys. Lett. B **592** (2004) 1.
- [45] Y. Goto *et al.* [Asymmetry Analysis collaboration], Phys. Rev. D **62** (2000) 034017 [arXiv:hep-ph/0001046].
- [46]
- [46] B. W. Filippone and X. D. Ji, Adv. Nucl. Phys. **26**, 1 (2001).